

# A Deep *ROSAT* HRI Observation of NGC 1313

Eric M. Schlegel<sup>1</sup>, Robert Petre<sup>2</sup>, E. J. M. Colbert<sup>2,3</sup>, Scott Miller<sup>3</sup>

## ABSTRACT

We describe a series of observations of NGC 1313 using the *ROSAT* HRI with a combined exposure time of 183.5 ksec. The observations span an interval between 1992 and 1998; the purpose of observations since 1994 was to monitor the X-ray flux of SN1978K, one of several luminous sources in the galaxy. No diffuse emission is detected in the galaxy to a level of  $\sim 1\text{--}2 \times 10^{37}$  ergs s<sup>-1</sup> arcmin<sup>-2</sup>. A total of eight sources are detected in the summed image within the D<sub>25</sub> diameter of the galaxy. The luminosities of five of the eight range from  $\sim 6 \times 10^{37}$  to  $\sim 6 \times 10^{38}$  erg s<sup>-1</sup>; these sources are most likely accreting X-ray binaries, similar to sources observed in M31 and M33. The remaining three sources all emit above  $10^{39}$  erg s<sup>-1</sup>. We present light curves of the five brightest sources. Variability is detected at the 99.9% level from four of these. We identify one of the sources as an NGC 1313 counterpart of a Galactic X-ray source. The light curve, though crudely sampled, most closely resembles that of a Galactic black hole candidate such as GX339-4, but with considerably higher peak X-ray luminosity. An additional seven sources lie outside of the D<sub>25</sub> diameter and are either foreground stars or background AGN.

*Subject headings:* Galaxies: spiral; stellar content

## 1. Introduction

One of the most significant discoveries using the *Einstein* Observatory was the existence in many nearby spiral galaxies of X-ray sources with luminosities in the range  $\sim 10^{39\text{--}40}$  erg s<sup>-1</sup>. As the brightest Galactic X-ray binary has an X-ray luminosity of a few  $\times 10^{38}$  erg s<sup>-1</sup>, these *Einstein* sources represented a new class. Some of these sources are located in the central regions of spirals (e.g., NGC 6946, IC 342, and the northern source in NGC 1313 (Fabbiano & Trinchieri 1987); M33 (Markert & Rallis 1983)), so they were originally believed to be low-activity active nuclei or starburst regions. Others, however, are well-separated from the galactic nucleus (e.g., the southern source in NGC 1313; Fabbiano & Trinchieri 1987) and could not be so easily explained.

With the more powerful X-ray observatory

*ROSAT*, higher-sensitivity observations of many nearby galaxies have been possible. In NGC 6946 (Schlegel 1994) and IC 342 (Bregman et al. 1993), the luminous nuclear regions have been resolved into an ensemble of discrete sources. In NGC 1313, the supposed nuclear source was shown to be located a full kiloparsec from the optical nucleus (Colbert et al. 1995; Colbert & Mushotzky 1999). While spectroscopic observations using the X-ray observatory *ASCA* have shown that the central source in M33 is not an active nucleus (Takano et al. 1993), the nature of the NGC 1313 “central” source remains undetermined.

NGC 1313 is a barred spiral galaxy (SBd; deVaucouleurs et al. (1991)) in the southern hemisphere. Its distance is estimated to be 4.5 Mpc (deVaucouleurs 1963). Numerous bright star-forming regions are present in the galaxy (Ryder et al. 1995). The only very luminous X-ray source optically identified is SN1978K, the first supernova identified as such on the basis of its X-ray emission (Ryder et al. 1993).

Using a set of *ROSAT* HRI observations obtained over the past 6 years, we have detected two

<sup>1</sup>High Energy Astrophysics Division, Smithsonian Astrophysical Observatory, Cambridge, MA 02138

<sup>2</sup>X-ray Astrophysics Group, Laboratory for High Energy Astrophysics, NASA-GSFC, Greenbelt, MD 20771

<sup>3</sup>Department of Astronomy, University of Maryland, College Park, MD 20742

additional highly luminous sources within 1 kpc of the nucleus. We find that all three central sources exhibit temporal variability, providing the first evidence that they are all compact. We also present the summed image of all of the individual observations which provides a deep look at NGC 1313.

## 2. Observations

Nine *ROSAT* HRI observations have been obtained over the years 1992-1998. Eight were collected as part of a monitoring program of SN1978K (Schlegel, Petre, & Colbert 1996; Schlegel et al. 1999); the ninth was obtained to pursue the optical identification of a different source (Stoche et al. 1994, 1995). The summary of the complete data set is contained in Table 1. A single *ROSAT* observation was typically spread across several calendar weeks; the MJD listed in the table is the value near the center of the observing window.

The data have all been reduced identically. Each observation was processed with the “extended source” software described by Snowden (1998) and available at the US *ROSAT* Science Data Center at NASA-GSFC. The software accounts for the particle background, filtering out times of anomalously high background and other bad quality data. Each observation was also corrected for the aspect error described by Harris (1999). This error arose from incorrect times (the fractional portion) that are associated with each aspect record which led to incorrect positions for each event. The data were affected because the point spread function was broadened by  $\sim 3''$ . The correction was applied to the first seven observations; the last two were unaffected by the error (the eighth and ninth observations had zero or nearly zero fractional times, so the error was at the level of  $\sim 0''.1$ , well below detectability). Once the data were filtered and aspect-corrected, the images from all of the observations were registered (using the IRAF/STSDAS task “registration”) and stacked. Figure 1 shows the resulting stacked image.

The *Chandra* Observatory source detection task “wavdetect,” based on the wavelet code of Micela et al. (1996), was used to locate point sources using a detection criterion of  $>4.5 \sigma$  (at most,  $<1$  false source). The detection threshold varies with off-axis angle. At the center, the threshold

is  $\sim 2 \times 10^{-4}$  counts  $s^{-1}$  which corresponds to a luminosity of  $\sim 5 \times 10^{37}$  ergs  $s^{-1}$  assuming a thermal spectrum of temperature 3 keV and absorbed by the known column density toward NGC 1313 ( $N_{\text{H}} \sim 6 \times 10^{20}$   $\text{cm}^{-2}$  from an  $E_{\text{B-V}}$  of 0.11 (Schlegel, Finkbeiner, & Davis 1998) and using the  $N_{\text{H}}-E_{\text{B-V}}$  relation of Predehl & Schmitt 1995). At a radius of  $10'$ , the threshold is  $\sim 2.5 \times 10^{-4}$  counts  $s^{-1}$  or  $\sim 7 \times 10^{37}$  ergs  $s^{-1}$ .

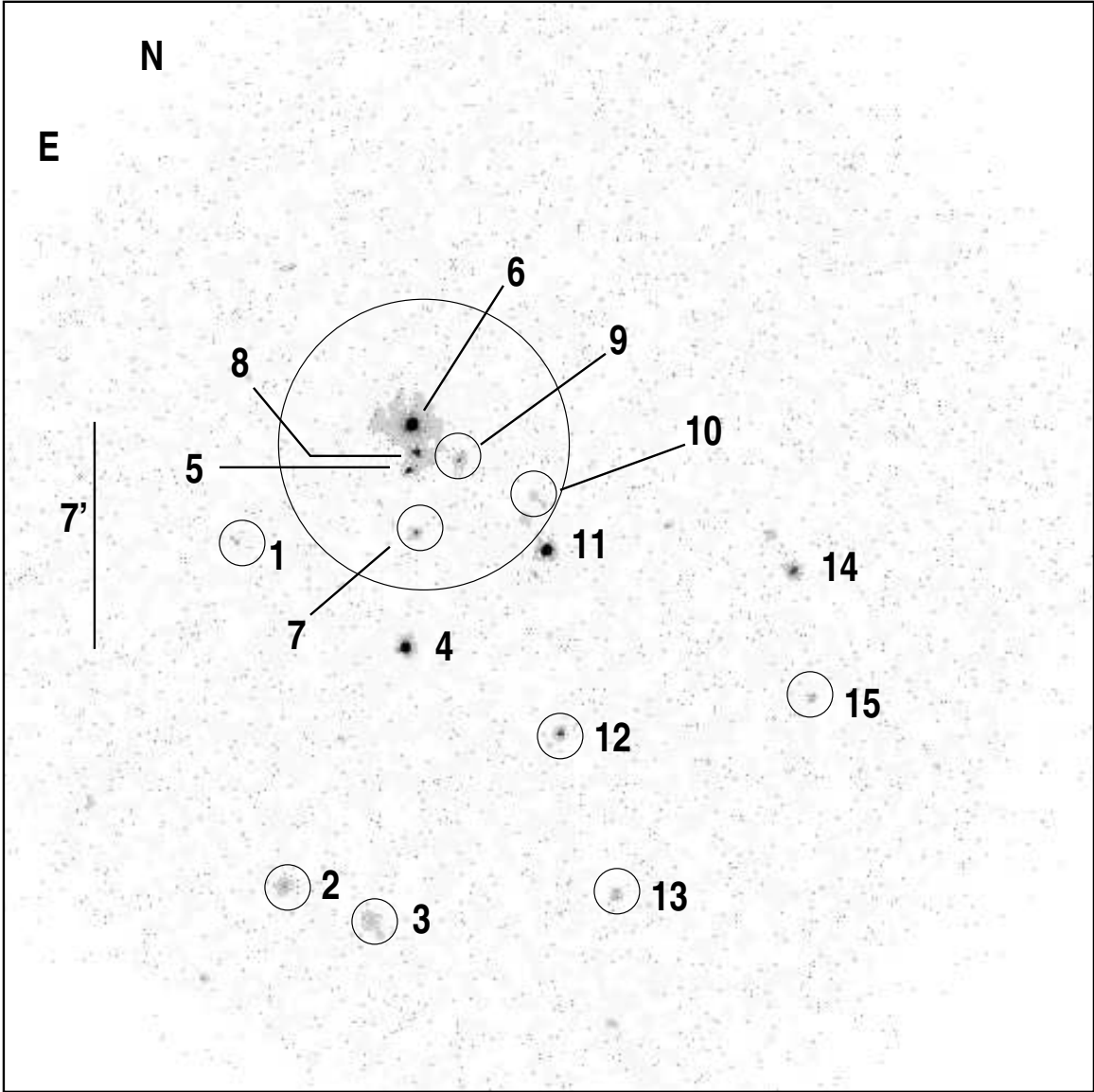
A total of 15 sources were found in the summed image; the detection task ignored any “source” within  $2'$  of the edge of the field where the vignetting is severe. The detected sources are listed in Table 2 with their positions (J2000), total exposure time at the source’s position, detected counts, estimated flux and luminosity, and PSPC counterpart name (Colbert et al. 1995; Miller et al. 1998). The sources are ordered by decreasing right ascension. For this paper, we number the sources and use the numbers for the source name instead of the longer but complete *ROSAT* source number.

We extracted the counts for each source using an aperture of  $40''$ , taking care to exclude counts from nearby sources. The background was extracted from an annulus surrounding the entire galaxy. The counts from any source falling within the background annulus were excluded. The vignetting within  $\sim 5'$  of the center is small ( $\sim 5\%$ ) but the correction was applied to any source with an off-axis angle  $>1'$ . No energy filtering was applied during the extraction, so the extracted counts represent the incident flux for the complete bandpass of the HRI (0.1–2.4 keV).

The HRI efficiency was relatively constant throughout the *ROSAT* mission. The HRI high voltage was increased to compensate for a loss of gain on 1994 June 21. As a consequence, the HRI flux sensitivity increased by  $\sim 10\%$ ; any sources showing fluctuations at or below the 10% level were interpreted as constant. As we describe below, the variability of several sources is too large to be interpreted as resulting from the gain change. Note, in particular, that all observations but the first occurred after the gain change.

The luminosity of each source is estimated assuming it is located within NGC 1313; several of the sources are likely to be foreground (or background) objects, so the true luminosity will be lower (or higher). The unabsorbed luminosities (Table 2) in the 0.1–2.4 keV band were estimated

Fig. 1.— Stacked image of NGC 1313 from nine separate epochs of *ROSAT* HRI observations. The total exposure time is  $\sim 182$  ksec at the center of the image. Source labels generally lie to the right of the source, except in the crowded region around the nucleus. Sources are listed in Table 2 in order of decreasing RA. Source 11 is SN1978K. Several of the weaker sources are circled for clarity. The largest circle schematically defines the  $D_{25}$  diameter ( $\sim 9'$ ).



by comparing the source count rates with that expected from a source with a thermal spectrum ( $kT = 2$  keV) and a column density identical to the Galactic column. For a column density of  $1.5 \times 10^{21} \text{ cm}^{-2}$ , the approximate mean value for  $N_{\text{H}}$  obtained from fitting the PSPC data of sources 6 (=X-1) and 4 (=X-2) (Colbert et al. 1995; Miller et al. 1998), the unabsorbed luminosities decrease by  $\sim 25\%$ . The luminosities differ by  $\sim 25\%$  if the adopted temperature is instead set to 7 keV. The luminosities also differ by  $\sim 10\text{-}15\%$  assuming other adopted thermal models at a temperature of 2 keV but differ by  $\sim 80\%$  for an adopted power law model. The power law is particularly sensitive to the column density value.

Figure 1 shows the composite image of NGC 1313. Except in the crowded region near the nucleus, the appropriate Table 2 label is placed directly beneath each source.

### 3. The Summed Image

Figures 2a and 2b show X-ray contours superposed on an optical image<sup>4</sup> of NGC 1313. The first figure shows the entire galaxy with the gray scale set at two different values: a “high” scaling and a “low” scaling. The second image shows the center of the galaxy with the contrast set to show the inner region. None of the sources lie on the bar. Source 6 falls just east of the northern end of the bar. Source 7 lies just east and approximately midway along the bar. Source 9 is positioned on the northern side of the west trailing arm. Source 5 lies  $\sim 1'$  east of the southern end of the bar. While all of the sources lie east of the bar, the positional match of source 11=SN1978K with its optical position ensures that the aspect solution is correct.

The deep image shows no evidence of diffuse emission across the face of the galaxy (diffuse emission may be present surrounding source 6, which we will discuss shortly). An adaptively-smoothed image, generated using a box size requiring a minimum of 99 counts, showed a circularly-symmetric image that resembled the exposure map. In other words, the adaptively-smoothed image is consistent with the expected

vignetting gradient. To assign an upper limit to the presence of diffuse emission, we extracted the counts in a circular aperture, centered on the galaxy, with a radius corresponding to half of its  $D_{25}$  diameter ( $\sim 9'$ , Tully (1988)). We excluded the counts for all point sources that fell within the aperture (sources 4 through 11). As a check on our procedure, we also extracted the blank region NW and S of NGC 1313. We corrected these off-axis regions for the difference in extracted areas and for the reduced exposure time resulting from vignetting. We corrected for the vignetting using the exposure map that is a product of the extended source software of Snowden (1998).

A net total of  $297 \pm 243$  counts was extracted within the on-galaxy aperture; the area encompassed on the sky is  $\sim 55.8 \text{ arcmin}^2$ . For a mean exposure time of 182.6 ksec across this region, the net counts correspond to a count rate of  $16.3 \pm 13.3 \times 10^{-4} \text{ cts s}^{-1}$ . Adopting the  $3\sigma$  upper limit of  $\sim 4 \times 10^{-3} \text{ counts s}^{-1}$ , the  $3\sigma$  upper limit on the luminosity in the 0.1–2.4 keV band is  $\sim 1 \times 10^{39} \text{ ergs s}^{-1}$  or  $\sim 1.5 \times 10^{37} \text{ ergs s}^{-1} \text{ arcmin}^{-2}$  across the extraction region. This limit is about a factor of 2 higher than the PSPC limit (Miller et al. 1998) of  $\sim 7 \times 10^{36} \text{ erg s}^{-1} \text{ cm}^{-2}$  (correcting an arithmetic error in that paper). The factor of 2 lies within 30% of the expected difference based on a calculation of the instrumental backgrounds and sensitivities between the PSPC and the HRI.

In Figure 1, diffuse emission appears to be concentrated around source 6. To examine whether this emission is truly diffuse, we extracted the counts from sources 6 and 4 in annuli centered on each source and extending outward to  $\sim 2'$ . Extraneous sources falling within the annuli were excluded. Source 4 is believed to be a point source without any extended or nearby emission (Stocke et al. 1994, 1995). The resulting radial profiles are shown in Figure 3. The background counts were extracted from an annulus surrounding the entire galaxy and are shown as a dashed line in each figure. The solid line in each figure shows the calibrated point spread function (David et al. 1997) using the data from a long exposure of HZ 43. We fit the PSF curve to the data in the  $5''\text{-}10''$  and  $30''\text{-}50''$  range. The fit yielded a  $\chi^2/\nu$  of 1.28 for 39 degrees of freedom (the PSF is defined in (David et al. 1997), so the fit is for the scale factor) which corresponds to a significance of  $\lesssim 85\%$

<sup>4</sup>Image obtained via Skyview facility at NASA’s HEASARC; original digitized from the UK Schmidt Telescope Southern Sky Survey

Fig. 2.— X-ray contours superposed on the digitized UK Schmidt Sky Survey image of NGC 1313. (a) the entire galaxy scaled for high grayscale values (left) and low grayscale values (right); (b) an expanded view near the nucleus, scaled to show the inner galaxy.

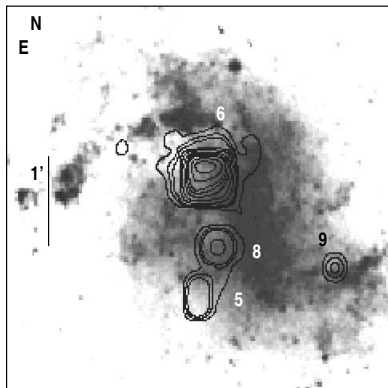
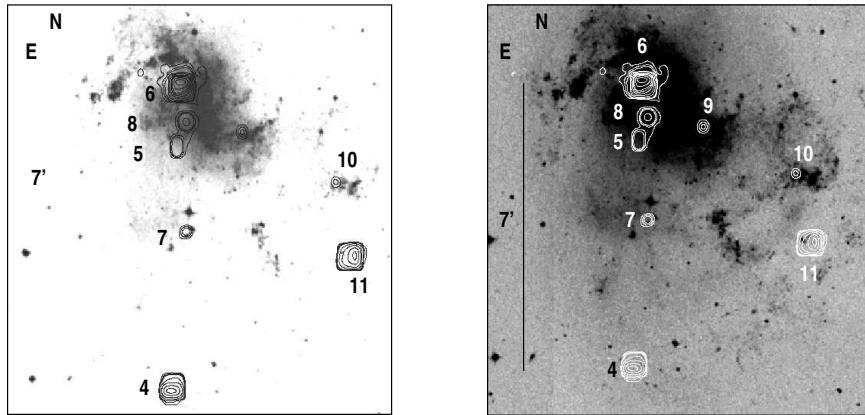
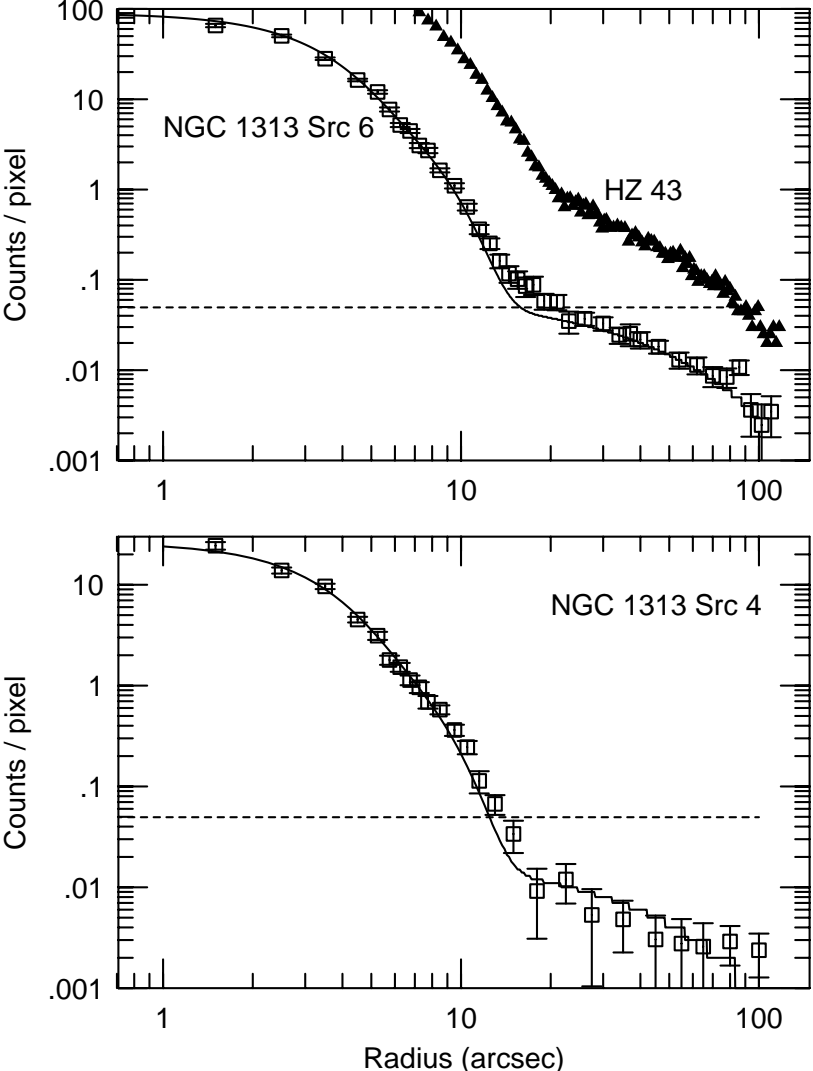


Fig. 3.— Azimuthally-averaged radial profiles centered on source 6 (top) and 4 (bottom) compared with the *ROSAT* HRI calibrated point spread function from HZ 43 David et al. (1997). The background level is indicated by the dashed line. The PSF profile of HZ 43 is included in the top figure (filled triangles) solely for comparison. Note the excess near 15-20'' in Source 6; the same behavior is visible in HZ 43 (David et al. 1997).



for any deviations from the model PSF. A fit to the HZ 43 profile yielded a similar significance.

Neither profile shows any evidence for extended emission when compared to HZ 43. The slight excess observed at the bend in the PSF at  $\sim 15$ – $18''$  is also visible in the HZ 43 data (David et al. 1997); the same few points near  $\sim 18''$  that lie above the functional form of the PSF in sources 4 and 6 also do so in the HZ 43 data. Beyond about  $20''$ , the known HRI halo begins to dominate. The visual impression of diffuse emission surrounding source 6 results solely from the long exposure that reveals the instrumental halo.

The nucleus of NGC 1313 is also not detected. Its position at 03:18:17.5, -66:29:48 (J2000, Ryder et al. (1995)), corresponds to an offset of about  $0'.6$  NW of source 8 in Figure 2b. We extracted the counts in an aperture centered on the nucleus and corrected them for the known halo surrounding source 6. These counts represent an upper limit on the flux at the nucleus and correspond to a  $3\sigma$  count rate of  $3.7 \times 10^{-4}$  counts  $s^{-1}$  or a flux of  $\sim 4 \times 10^{-14}$  ergs  $s^{-1}$   $cm^{-2}$ . At the distance of NGC 1313, the luminosity is  $\sim 9 \times 10^{37}$  ergs  $s^{-1}$  in the 0.1–2.4 keV band.

#### 4. The Sources

Before launching into a description of the individual sources, we first comment on the sources *en masse*. Sources 1, 2, 3, 12, 13, 14, and 15 lie outside of the  $D_{25}$  region of NGC 1313 and are very likely not associated with the galaxy. We describe them briefly in the appendix. From the *ROSAT* log N-log S relation Hasinger et al. (1994), we estimate a total of  $\sim 4$ – $6$  extragalactic sources lie within the HRI field-of-view. Within the  $D_{25}$  radius, we expect  $\sim 0.2$ – $0.4$  extragalactic sources. Both estimates provide support for the comment that the seven sources are external to NGC 1313.

For the sources detected by both the PSPC and the HRI, the HRI positions agree to within  $\sim 10''$  with the PSPC positions presented in Colbert et al. (1995); Miller et al. (1998). These positional uncertainties are typical of PSPC positions.

The luminosity estimated for source 11 (= SN1978K) agrees with the luminosity estimate obtained from the PSPC data to better than  $\sim 15\%$ . Source 11 is the only approximately constant source in NGC 1313 during the years of ob-

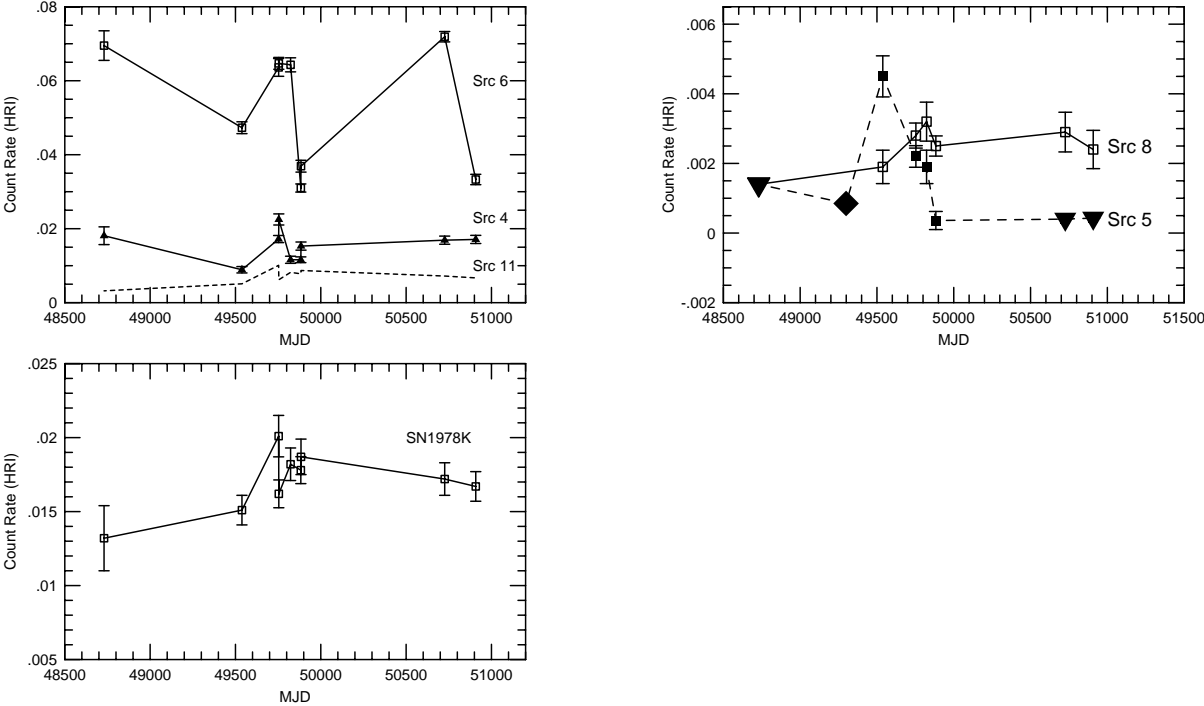
servation. The luminosity estimates for sources 4, 6, 10, and 14 differ by factors ranging from  $\sim 0.2$ – $0.3$  (sources 4 and 6) to  $\sim 0.5$  (sources 10 and 14). We believe these differences are dominated by the variability of the sources (described below). For two of the weaker sources (7 and 8), the estimates differ by a factor of two. We estimate the fluxes can change by  $\sim 25\%$  if a model with an incorrect temperature is adopted.

The luminosity of source 9 differs from the luminosity measured in the two PSPC observations by a factor of  $\sim 4$ . If we estimate the expected HRI count rate by reducing the PSPC count rate by the PSPC-to-HRI count conversion factor of  $\sim 2.5$ , we estimate the summed HRI image should yield  $109 \pm 21$  counts. Instead, we detect only  $38 \pm 11$  counts; the difference is significant at the  $>99\%$  level and establishes source 9 as a variable object. The PSPC data sets show essentially no differences in the count rates between the two observations in 1991 and 1993. The “variability” must then be a long-term change that operates over a scale of years.

We have searched for variability of the sources using the HRI data sets. In Table 3, we summarize the data and the results of this search. For each source we list the count rate or upper limit for each observation. For the weaker sources, we have added together adjacent observations to improve the significance of some of the detections. We have performed a chi-squared test against the hypothesis of constant source flux, using the average detected flux. By ignoring upper limits, we obtain a chi-squared that represents a conservative estimate of the likelihood of source variability. As can be seen from Table 3, sources 4, 5, 6, 8, and 11 all are variable with high probability ( $>97$  percent).

Source 6 (= X-1 in Colbert et al. (1995); Miller et al. (1998)) is located near the northern end of the bar (Colbert et al. 1995). Studies by Ryder et al. (1995) and Peters et al. (1993) indicate that it lies north of the dynamical and photometric center of NGC 1313 by  $\sim 1$  kpc ( $\sim 40''$ ). There is no known counterpart, in either the optical or the radio. Colbert & Mushotzky (1999), in a survey of nearby galaxies, show that about half of the nearby galaxies have a luminous source located just off of the dynamical center of the galaxy. Source 6 is the most luminous source in

Fig. 4.— HRI light curves covering the nine epochs of observations (a) sources 4 and 6 (solid lines), and source 11 = SN1978K (as a dashed line) (top) and source 11 (bottom). Note that the scale for the bottom plot covers 1/4 of the range of the top plot. (b) light curves for the sources 5 and 8. The upside-down triangles represent upper limits. The diamond on the light curve of source 5 is the 90% upper limit on the flux of source 5 in the *ROSAT* PSPC observation Miller et al. (1998).





the *ROSAT* band in NGC 1313, with  $L_X \sim 2 \times 10^{40}$  ergs  $s^{-1}$ . It was one of the two sources detected in the 1980 *Einstein* IPC observation (Fabbiano & Trinchieri 1987). There has been little evidence that it varies other than the two PSPC observations which were separated by more than two years (Miller et al. 1998). The HRI variability (Figure 4, top) is a crucial piece of evidence on the source size, namely, it must be compact having undergone a factor of 2 change in  $\lesssim 60$  days (near MJD 49850). From the light travel time, 60 days corresponds to a physical size  $< 0.05$  pc. The variability, luminosity, and spectrum (Colbert et al. 1995; Petre et al. 1994a,b) suggest it is an active nucleus-like source with a mass of  $\sim 10^{3-4} M_\odot$  while the lack of a counterpart and the displacement from the nucleus provide evidence against this hypothesis and simultaneously testifies to its unusual nature.

Source 4 (= X-2 in Colbert et al. (1995); Miller et al. (1998)), the other source detected in the IPC observation (Fabbiano & Trinchieri 1987), has been thought by some to be a nearby Galactic source, perhaps a cooling neutron star (Stoche et al. 1994, 1995). The *ASCA* SIS data, however, indicate that the X-ray spectrum is not that expected for a cooling neutron star ( $T \sim 10^6$  K), but is more typical of a low-mass X-ray binary: a thermal spectrum with  $kT \sim 2$  keV (Petre et al. 1994a,b). Unlike source 6, intensity variability was detected from it between the 1980 IPC and the 1991 PSPC observation (Colbert et al. 1995). Colbert et al. argue that the source is a black hole candidate with a mass of  $> 100 M_\odot$  based upon its PSPC + IPC spectrum and its super-Eddington luminosity.

The X-ray luminosity of SN1978K (= source 11 in this paper = X-3 in Colbert et al. (1995); Miller et al. (1998)); Ryder et al. (1993)) is formally variable at the 97% confidence level across the 9 HRI observations (Figure 4, bottom). The largest flux change from the mean of the 9 observations is  $\sim 23\%$ . Schlegel, Petre, & Colbert (1996), however, stated that SN1978K was constant within the errors. We reconcile these statements by recalling that the  $\chi^2$  estimate tests for variability within the observation set. For SN1978K, however, we are also interested in whether a trend exists for the entire data set. Essentially, the 97% variability can be considered as the “micro-variability;” the long-

term trend would then be the “macro-variability.” The details of the fit to the light curve are described in Schlegel et al. (1999). Very briefly, the X-ray luminosity should decay as  $L \propto t^\alpha$ . A fit to the data gives  $\alpha = (-3.71 \pm 6.52) \times 10^{-5}$  (90% confidence range). In other words, there is no decay, so the long-term luminosity is constant within the errors. The luminosity did increase by at least a factor of 5 from 1980, when it was not detected by the *Einstein* IPC (1.5 years after optical maximum) to its discovery in 1991 with the *ROSAT* PSPC (Ryder et al. 1995; Schlegel, Petre, & Colbert 1996). We refer readers to the cited papers for details.

One other supernova has appeared in NGC 1313: SN1962M. At the position of SN1962M (03:18:15,-66:29:51 J2000), we extracted  $29.5 \pm 11.6$  counts which corresponds to a  $3\sigma$  flux of  $\sim 2.5 \times 10^{-14}$  ergs  $s^{-1} cm^{-2}$  or a corresponding luminosity upper limit of  $\sim 5 \times 10^{37}$  ergs  $s^{-1}$ . There is no evidence that SN1962M has been detected.

The remaining sources may be accreting X-ray binaries similar to sources detected in M31 and M33. Source 8 appears to be a relatively steady X-ray source, perhaps a persistent X-ray binary with a luminosity of  $\sim 6 \times 10^{38}$  ergs  $s^{-1}$  (Figure 4b). Miller et al. (1998) showed that the hardness ratio, defined as  $(H-S)/(H+S)$ , with  $H$  = photons with energies  $> 1$  keV and  $S$  = photons with energies  $< 1$  keV, is  $+0.26$ . For a source with that hardness absorbed by the known Galactic column density, a thermal bremsstrahlung spectrum must have  $kT \gtrsim 2$  keV.

Source 5 may be the most dramatic source (Figure 4b). No source was detected in the first HRI observation, but the exposure time was sufficiently short that the upper limit is not particularly restrictive. The second HRI exposure shows an easily detected source. This exposure occurred after the gain change. The increase in flux of source 5 is not only substantially larger than the  $\sim 10\%$  change in sensitivity, but it also is not matched by the other sources. Sources 4 and 6 became considerably fainter in the second observation; sources 7 and 11 brightened slightly (and perhaps consistently with the increased sensitivity from the gain change). Subsequent exposures show source 5 fading by about a factor of 10 in  $\sim 300$  days. When the full light curve is accumulated, it is easy to conclude that an outburst occurred near the time

of the second exposure. The increase in flux is at least a factor of 3, from  $L_X \sim 3 \times 10^{38}$  to  $\sim 10^{39}$  ergs  $s^{-1}$ . We also included the PSPC observation described in Miller et al. (1998) because it falls near the time of brightening. No PSPC source is detected at the location of source 5; the plotted flux is the 90% flux upper limit for source 5. The flux was converted to an HRI count rate assuming a thermal bremsstrahlung spectrum absorbed by the Galactic column to NGC 1313.

Most X-ray transients do not reach  $L_X \sim 10^{39}$  erg  $s^{-1}$  levels unless the source is an X-ray binary (e.g., White, Nagase, & Parmar 1995). A supernova could produce the light curve. The presence of SN1978K guarantees considerable scrutiny of NGC 1313. Observations were made at MJD 49361 (day -177) and 49722 (day +184) in the optical; radio observations were obtained on MJD 49284 (day -254) and 49627 (day +89) (Schlegel et al. 1999). We judge it unlikely a supernova could explode and fail to be reported. In the discussion to follow, we assume source 5 is a binary X-ray transient.

To compare the source's outburst to the X-ray light curves of known Galactic X-ray sources, we examined the 2-10 keV light curves obtained with the *RXTE* All-Sky Monitor. Ideally, a comparison should be made using X-ray binaries observed with the HRI. Few have been observed because of the high column density toward the Galactic center, and none monitored over a duration comparable to the NGC 1313 observations. The known column density to NGC 1313 is relatively low, as measured in the PSPC spectrum of source 6 (Colbert et al. 1995; Miller et al. 1998). On the basis of the column density, we estimate the mean energy of the source 5 photons to be  $\gtrsim 1.2$  keV, so the ASM light curves provide an approximate comparison to the HRI band. A precise comparison is not the goal; we are interested in whether any of the known Galactic X-ray transients have light curve shapes similar to that of source 5.

We arbitrarily assume the source 5 outburst occurred at or shortly before the time of the second exposure and set that time as the time of maximum. We downloaded ASM data from the accumulating database<sup>5</sup>. We extracted times

<sup>5</sup>The data are available from the *RXTE* WWW site at NASA-GSFC or the *RXTE* ASM site at MIT.

and fluxes surrounding bursts for the sources XTEJ1550-56, GX339-4, GRS1915+105, X0115+634, Aql X-1, and X1705-44. We then subtracted the minimum flux, scaled the data to the maximum, and subtracted the date of maximum. We smoothed the ASM data with a 5-point triangular response to reduce the point-to-point fluctuations and aid the visibility. No corrections for distance or column density have been made. Figure 5(a) shows the comparison between source 5's light curve and the light curves of XTEJ1550-56 and GX339-4 (top), GRS1915+105 and X0115+634 (bottom); Figure 5(b) shows the comparison to Aql X-1 and X1705-44.

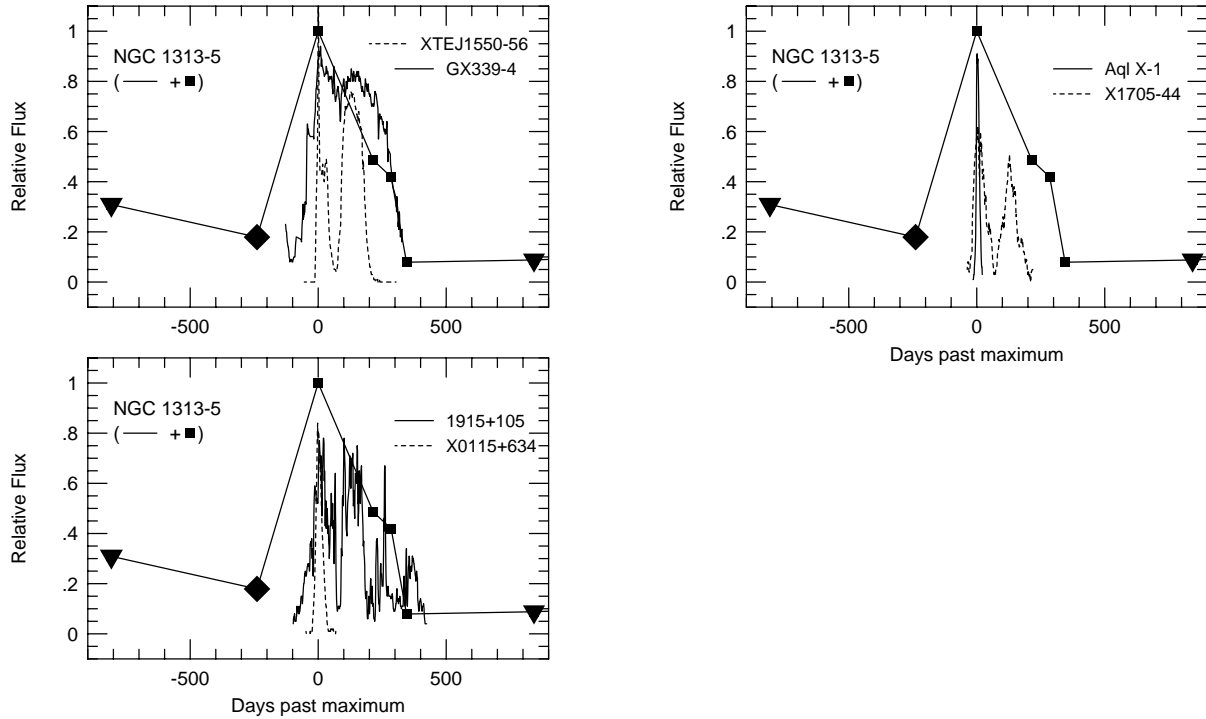
The source 5 light curve clearly possesses an outburst duration of several hundred days. The FWHM, assuming an infinite rise at day zero, is  $\sim 200$  days. Most Galactic X-ray transients have considerably shorter outbursts. For example, the FWHM of the outbursts of Aql X-1 and X0115+634 are  $\sim 10$  and  $\sim 20$  days, respectively. The FWZI width for Aql X-1 and X0115+634 are  $\sim 30$  and  $\sim 50$  days, respectively. The outburst duration for source 5 is much longer, even if we missed the maximum by  $\sim 100$  days.

We can not eliminate the possibility that multiple outbursts occurred in source 5 between the day 0 and day 220 HRI observations. Another possibility assumes the day 0 and subsequent points are the decay of a *second* outburst in a multiple-outburst sequence. The first outburst would then fit into the unobserved  $\sim 200$  day gap prior to the first detection.

If such an outburst did occur earlier, so that the second observation fell on an exponential decay curve (as is approximately shown by the XTEJ1550-56 curve), then source 5 must have been considerably brighter. By sliding the J1550 curve vertically and horizontally to a negative "age," the observed points can be made to fall at least close to the J1550 tail of the second burst. The FWZI is not reproduced unless we stretch the J1550 light curve. We have other examples of X-ray light curves that do not require such stretching.

The light curve for GX339-4 provides a good match to the data points, not only matching the width but also the steep decline at the end of the burst. If a match in light curve shape dictates physics, then by analogy with GX339-4, source 5

Fig. 5.— NGC 1313 source 5 HRI light curve compared to Galactic X-ray source light curves for XTE J1550-56, GX339-4, GRS1915+105, X0115+634, Aql X-1, and X1705-44. The data points all belong to source 5. Upper limits are shown by triangles with apex pointing down. The diamond is the PSPC observation from Miller et al. (1998). The light curves of the X-ray binaries have been smoothed (with a 5-point triangular response) solely for clarity.



is a black hole candidate. A highly variable source such as GRS1915+105 also can in principle provide a match to the light curve of source 5; the data do not have the time resolution to refute this possibility. Interestingly, GRS1915+105 is also a black hole candidate.

## 5. Discussion

NGC 1313 is not a particularly unusual galaxy. Its most distinctive attributes are a low metallicity and a high density of H II regions along the bar (Ryder et al. 1995). There is no evidence of nuclear activity, nor does it show any evidence of rapid star formation, past or present, despite having possibly interacted with its nearby companion, NGC 1313A (Sandage & Brucato 1979).

Three key issues are raised by the *ROSAT* data of NGC 1313: the lack of diffuse emission, the lack of a nuclear source, and the presence of several luminous sources. The lack of diffuse emission was discussed in Miller et al. (1998) and will not be repeated here. Essentially, a larger database of normal galaxies covering a broad range of properties is needed to place the presence or absence of diffuse emission in context. We note, however, that low-mass galaxies appear to contain holes in their neutral ISMs (e.g., Walter 1999). The holes may provide a channel by which injected energy escapes the ISM, rather than heating it. While that argument can explain the lack of a hot ISM in many dwarf galaxies, the H I layer in NGC 1313 does not appear to be dominated by holes (e.g., Ryder et al. 1995).

The absence of a nuclear source might indicate enhanced absorption surrounding the nucleus. If we assume the nuclear source is similar to source 6, the required column density to hide its X-ray emission and yield our observed upper limit is about  $10^{23} \text{ cm}^{-2}$  which corresponds to an  $A_V \sim 45$ , too high to be detectable in the optical. If enhanced absorption does explain the non-detection of a nuclear source, an observation with *Chandra* or *XMM* may reveal it at  $E > 3\text{-}4 \text{ keV}$ .

A  $1 M_\odot$ , zero metallicity accreting source generates an Eddington luminosity of  $\sim 1.4 \times 10^{38} \text{ ergs s}^{-1}$ . In NGC 1313, excluding SN1978K, there are 5 sources above  $L_{\text{Edd}}$  (sources 4, 5, 6, 7, and 8). An overestimate of the distance will lower the luminosities; if, however, we believe the luminosities

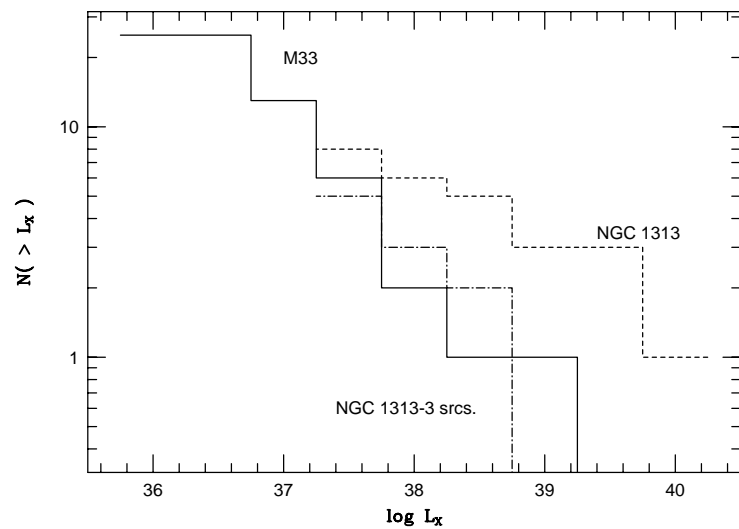
must be sub-Eddington, the distance then must be in error by a factor of two or more. Given the proximity of the galaxy and the amount of study it attracts, a distance error of that magnitude is very unlikely.

While sources with similar luminosities to the NGC 1313 sources are found in other nearby galaxies, for none of them does a Galactic counterpart exist. Sources of comparable luminosity can be found in, for example, M51 (Marston et al. 1995), M82 (Collura et al. 1994), M33 (Takano et al. 1993), and M101 (Wang, Immler, & Pietsch 1999). The two in M82 discussed by Collura et al. are of particular interest, as both show strong variability, and one has an average *ROSAT* band luminosity of at least  $5 \times 10^{39} \text{ ergs s}^{-1}$ , making it an X-ray binary candidate of comparable luminosity to the ones found in NGC 1313. Wang, Immler, & Pietsch (1999) discuss the number of luminous X-ray sources in several nearby galaxies and argue that the number of sources is correlated with the far-IR luminosity,  $L_{\text{FIR}}$ .  $L_{\text{FIR}}$  for NGC 1313 is 42.73, using the Devereux & Eales (1989) relation contained in the notes to their Table 7 and IRAS 60 and 100  $\mu$  fluxes from the NASA Extragalactic Database<sup>6</sup>. For NGC 1313, the  $L_{\text{FIR}}$  places it near the bottom of the range (slightly above M33). The  $L_X$  or, equivalently, the number of superluminous sources, places NGC 1313 nearer the top of the range.

If we eliminate the most luminous three objects from the luminosity distribution, the result resembles the distribution for M33 (Figure 6), an argument in favor of the interpretation that sources 5, 7, 8, 9, and 10 are accreting X-ray binaries. We can argue that the presence of SN1978K is fortuitous; over typical galactic times, its existence is ephemeral and happens to be visible at present. The other two sources, however, appear to be long-lived, particularly the near-nuclear source. We can ask how NGC 1313 has produced a top-heavy luminosity distribution. No explanation for the “overabundance” of very luminous X-ray sources readily presents itself. The existence of apparently super-Eddington non-nuclear sources in nearby galaxies, coupled with the lack of them in our Galaxy, is a long standing mystery in X-ray astronomy (Fabbiano 1998).

<sup>6</sup> Available from <http://nedwww.ipac.caltech.edu/>

Fig. 6.— The HRI luminosity distribution of sources for NGC 1313 compared to the distribution for M33. The solid and dashed lines represent the as-observed distributions for M33 and NGC 1313, respectively. The dot-dashed line represents the distribution for NGC 1313 if the three most luminous sources are removed.



### A. Serendipitous Sources in the NGC 1313 Field

Sources 1, 2, 3, 12, 13, 14, and 15 lie outside of the  $D_{25}$  circle centered on the galaxy. Sources 4 and 11 = SN1978K also lie outside that radius. SN1978K is definitely associated with NGC 113. The distance to source 4 is less certain (Stoche et al. 1994, 1995; Petre et al. 1994a,b). We used the APM WWW site (<http://www.ast.cam.ac.uk/~apmcat/>) to list potential optical counterparts. From the APM list, we obtained a magnitude and using the nomogram of Maccacaro et al. (1988), estimated a  $\log(f_X / f_V)$  value. A single counterpart fell within  $4''$  of the HRI position for sources 1, 2, 12, 14, and 15. For sources 3 and 13, the offsets were larger ( $9''$  and  $7''$ , respectively). All of the objects are fainter than mag 20.0 and all appear to be point sources. The nomogram indicates all are AGN or BL Lac objects. Table 4 lists the sources, the closest optical counterpart, its magnitude, and the nomogram.

EMS thanks Jeff McClintock for a pointer to the literature on the light curves of X-ray binaries. This research was supported by NASA grant NAG5-4015 to the Smithsonian Astrophysical Observatory.

## REFERENCES

- Bregman, J., Cox, C., & Tomisaka, K. 1993, *ApJ*, 415, L79
- Colbert, E. J., Petre, R., Schlegel, Eric M., & Ryder, S. 1995, *ApJ*, 446, 177
- Colbert, E. J. & Mushotzky, R. M. 1999, *ApJ*, 519, 89
- Collura, A., Reale, F., Schulman, E., & Bregman, J. 1994, *ApJ*, 420, L63
- David, L., Harnden, F. R., Jr., Kearns, K., & Zombeck, M. V. 1997, *The ROSAT High Resolution Imager (HRI) Calibration Report* (rev. ed., Cambridge: US *ROSAT* Science Data Center)
- de Vaucouleurs, G., de Vaucouleurs, A., Corwin, H. G., Buta, R., Paturel, G., & Fouqué, P. 1991, *Third Reference Catalog of Bright Galaxies* (New York: Springer-Verlag)
- de Vaucouleurs, G. 1963, *ApJ*, 137, 720
- Devereux, N. A. & Eales, S. A. 1989, *ApJ*, 340, 708
- Fabbiano, G. 1998 in *The Hot Universe*, ed. K. Koyama, S. Kitamoto, & M. Itoh (Dordrecht: Kluwer Academy Publ), 93
- Fabbiano, G. & Trinchieri, G. 1987, *ApJ*, 315, 46
- Harris, D. 1999, *Bull AAS*, 31:2, 719
- Hasinger, G., Burg, R., Giacconi, R., Hartner, G., Schmidt, M., Truemper, J., & Zamorani, G. 1994, *A&A*, 291, 348
- Maccacaro, T., Gioia, I., Wolter, A., Zamorani, G., & Stocke, J. 1988, *ApJ*, 326, 680
- Markert, T. H. & Rallis, A. D. 1983, *ApJ*, 275, 571
- Marston, A. P., Elmegreen, D. M., Elmegreen, B., Forman, W., & Jones, C. 1995, *ApJ*, 438, 663
- Micela, G., Sciortino, S., Kashyap, V., Harnden, Jr., F. R., & Rosner, R. 1996, *ApJS*, 102, 75
- Miller, S., Schlegel, Eric M., Petre, R. & Colbert, E. J. 1998, *AJ*, 116, 1657
- Peters, W., Freeman, K., Forster, K., Manchester, R., & Ables, J. 1993, *MNRAS*, 269, 1025
- Petre, R., Schlegel, E., Colbert, E., Okada, K., Makishima, K., & Mihara, T. 1994a, in *New Horizons in X-ray Astronomy*, eds. F. Makano & T. Ohashi (Tokyo: Universal Academy Press), 519
- Petre, R., Okada, K., Mihara, T., Makishima, K., & Colbert, E. J. 1994b, *PASJ*, 46, L115
- Predehl, P. & Schmitt, J. H. M. M. 1995, *A&A*, 293, 889
- Ryder, S., Staveley-Smith, L., Dopita, M., Colbert, E. J., Petre, R., Malin, D., & Schlegel, E. M. 1993, *ApJ*, 416, 167
- Ryder, S., Staveley-Smith, L., Malin, D. F., & Walsh, W. 1995, *AJ*, 109, 1592
- Sandage, A. & Brucato, R. 1979, *AJ*, 84, 472
- Schlegel, Eric M. 1994, *ApJ*, 434, 523
- Schlegel, Eric M., Petre, R., & Colbert, E. J. 1996, *ApJ*, 456, 187
- Schlegel, Eric M. et al. 1999, *AJ*, 118, 2689
- Schlegel, D. J., Finkbeiner, D., & Davis, M. 1998, *ApJ*, 500, 525
- Snowden, S. L. 1998, *ApJS*, 117, 233
- Stocke, J., Wang, Q. D., Perlman, E., Donahue, M., & Schachter, J. 1995, *AJ*, 109, 1199
- Stocke, J., Wang, Q., Perlman, E., Donahue, M., & Schachter, J. 1994, in *The Soft X-ray Cosmos*, ed. E. Schlegel & R. Petre (New York: AIP), 75
- Takano, M., Mitsuda, K., Fukazawa, Y., & Nagase, F. 1993, *ApJ*, 436, L47
- Tully, R. 1988, *Nearby Galaxies Catalog*, (Cambridge: Cambridge University Press)
- Walter, F. 1999, *PASA*, 16, 106
- Wang, Q. D., Immler, S., & Pietsch, W. 1999, *ApJ*, 523, 121
- White, N., Nagase, F., & Parmar, A. 1995 in *X-ray Binaries*, ed. W. Lewin, (Cambridge: Cambridge University Press), 1

Table 1: *ROSAT* HRI Observations

Sequence	Observation Date	MJD	Exposure Time (sec)	Pointing centered on
400065n00 <sup>a,b</sup>	1992 Apr 18-May 24	48730	5365	NGC 1313
600505n00 <sup>a</sup>	1994 Jun 23-Jul 16	49538	22199	NGC 1313
500403n00	1995 Jan 31-Feb 10	49753	13314	SN1978K
500404n00	1995 Feb 2-11	49754	26898	SN1978K
600505a01	1995 Apr 12-20	49823	20143	NGC 1313
500403a01	1995 May 10-Jul 22	49883	30736	SN1978K
500404a01	1995 May 9-Jul 21	49884	18628	SN1978K
500492n00	1997 Sep 30-Aug 10	50726	22537	SN1978K
500499n00	1998 Mar 21-Apr 20	50908	23754	SN1978K

<sup>a</sup>In light curve presented in Schlegel, Petre, & Colbert (1996).

<sup>b</sup>Data described in Stocke et al. (1994) or Stocke et al. (1995).

Table 2: Detected Sources in Summed Image

Number	J2000		Total ExpT (sec)	Cts/sec ( $\times 10^4$ )	Flux <sup>a</sup>	L <sub>X</sub>	Old Label <sup>b</sup>
	RA	Dec					
1	3:19:14.7	-66:32:46.0	177241	12.1 $\pm$ 1.3	1.3 $\pm$ 0.2(-13)	3.1(38)	X12 <sup>c</sup>
2	3:19:01.0	-66:43:26.4	167992	6.9 $\pm$ 1.0	7.3 $\pm$ 0.1(-14)	1.8(38)	new
3	3:18:34.8	-66:44:27.1	169763	4.8 $\pm$ 0.9	5.1 $\pm$ 0.9(-14)	1.2(38)	new
4	3:18:22.0	-66:36:02.3	182585	149.0 $\pm$ 3.5	1.6 $\pm$ 0.04(-12)	3.9(39)	X2
5	3:18:21.0	-66:30:32.3	182878	13.8 $\pm$ 1.6	1.4 $\pm$ 0.2(-13)	3.4(38)	new
6	3:18:20.2	-66:29:07.3	181387	515.9 $\pm$ 5.8	5.4 $\pm$ 0.06(-12)	1.3(40)	X1
7	3:18:18.9	-66:32:29.9	183675	5.9 $\pm$ 0.8	6.2 $\pm$ 0.8(-14)	1.5(38)	X8
8	3:18:18.5	-66:30:02.3	182693	25.5 $\pm$ 1.7	2.7 $\pm$ 0.2(-13)	6.5(38)	X6
9	3:18:06.0	-66:30:12.4	184064	2.1 $\pm$ 0.6	2.2 $\pm$ 0.6(-14)	5.3(37)	X7
10	3:17:42.7	-66:31:22.5	184757	2.1 $\pm$ 0.6	2.2 $\pm$ 0.6(-14)	5.3(37)	X11
11	3:17:38.4	-66:33:02.5	182739	171.6 $\pm$ 3.7	1.8 $\pm$ 0.04(-12)	4.3(39)	X3
12	3:17:35.0	-66:38:42.5	176697	13.7 $\pm$ 1.2	1.4 $\pm$ 0.1(-13)	3.4(38)	X10
13	3:17:16.4	-66:43:47.3	172713	8.4 $\pm$ 2.2	8.8 $\pm$ 2.3(-14)	2.1(38)	new
14	3:16:22.1	-66:33:41.0	181503	8.1 $\pm$ 0.9	8.5 $\pm$ 0.9(-14)	2.1(38)	X9
15	3:16:16.8	-66:37:40.8	172503	3.3 $\pm$ 0.7	3.5 $\pm$ 0.7(-14)	8.4(37)	new

<sup>a</sup>Flux in the 0.1–2.4 keV band calculated assuming unabsorbed 2 keV thermal bremsstrahlung spectrum with  $N_{\text{H}} = 6 \times 10^{20}$  cm<sup>-2</sup>. This assumes all of the objects are in NGC 1313 ( $D = 4.5$  Mpc); for objects not in NGC 1313, this procedure will underestimate the flux by  $\sim 30\%$  for a source at a distance of 1 kpc. The percent change in  $L_{\text{X}}$  is  $\sim 25\%$  for  $N_{\text{H}} = 1.5 \times 10^{21}$  cm<sup>-2</sup>.

<sup>b</sup>labels used in Colbert et al. (1995) and Miller et al. (1998).

<sup>c</sup>Detected in Miller et al. (1998) but not discussed; not detected in Colbert et al. (1995)



Table 3: Count Rates of NGC 1313 Sources<sup>a</sup>

MJD	Source Number							
	4	5	6	8	9	11	12	14
48370	18.1±2.4	<1.4	69.8±4.0	<1.4	<1.4	13.1±2.1	<1.4	<1.5
49538	9.8± 0.9	4.4±0.6	46.5±1.6	1.9±0.5	1.5±0.6	15.0±1.0	0.8±0.6	0.9±0.6
49753	22.6±1.5	6.7±0.9	64.6±2.4	8.5±1.1	4.1±1.3	20.2±1.5	2.0±1.2	2.6±1.3
49754	17.2±1.0	–	65.8±1.7	–	–	16.3±1.0	–	–
49823	11.7±1.0	1.9±0.5	63.7±1.9	3.2±0.5	<0.6	17.2±1.1	<0.6	<0.7
49883	11.5±0.8	0.6±0.4	30.8±1.6	4.0±0.5	1.8±0.7	18.0±0.9	1.7±0.7	2.7±0.7
49884	15.2±1.1	–	36.5±1.6	–	–	18.8±1.2	–	–
50726	16.5±1.0	<0.4	71.5±1.9	2.8±0.6	1.8±0.6	17.3±1.1	2.0±0.6	1.6±0.6
50908	17.3±1.1	<0.4	33.0±1.3	2.3±0.5	1.5±0.6	16.8±1.1	0.7±0.6	0.8±0.6
Chi-squared	16.1	11.8	125.	7.8	0.9	2.1	0.6	1.0
Probability	>0.999	>0.999	>0.999	>0.999	0.55	0.97	0.20	0.55

<sup>a</sup>Count rates in units of  $10^{-3} \text{ s}^{-1}$

Table 4: Description of Serendipitous Sources

Source	Closest Optical Counterpart		X-ray - Optical		
	RA	Dec	Mag	offset	$\log(f_x / f_V)$
1	03:19:16.44	-66:32:45.9	0'' .8	21.0	+0.88
2	03:19:00.34	-66:43:25.8	1'' .9	20.2	+0.30
3	03:18:33.55	-66:44:27.3	9'' .0	22.1	+0.94
12	03:17:34.31	-66:38:41.9	2'' .1	22.2	+1.40
13	03:17:16.84	-66:43:40.9	7'' .1	20.5	+0.50
14	03:16:22.29	-66:33:40.2	1'' .5	20.0	+0.30
15	03:16:16.66	-66:37:37.5	3'' .6	21.6	+0.55

